OVERLAID PARALLEL COUPLED INSET DIELECTRIC GUIDES FOR BROADBAND APPLICATIONS TO DIRECTIONAL COUPLERS

Z. Fan and Y.M.M. Antar

Dept. of Electrical and Computer Engineering
Royal Military College, Kingston, ON K7K 5L0, Canada

Abstract

Overlaid parallel coupled inset dielectric guides are proposed for broadband applications to directional couplers, and analyzed by using the integral equation formulation and Galerkin's procedure. Results are presented to illustrate effects of thickness and dielectric constant of the overlay on propagation and coupling characteristics. It is found that by suitable choice of these parameters very flat coupling can be achieved for a wide frequency range.

I. Introduction

Studies of the aspect ratio and multilayer dielectric filling of the single inset dielectric guide (IDG) have shown that the one–layer structure can offer wider bandwidth than a rectangular waveguide and two–layer one may have very wide bandwidth exceeding that of a ridge waveguide [1]. It has also been demonstrated that optimum flat coupling between two parallel coupled IDGs exists for a certain value of the aspect ratio [2]. Through combining the single IDG with microstrips, both strong and weak directional couplers have been realized [3]. Two parallel coupled IDGs can also be used to design directional couplers. Very low return loss and high isolation for this kind of couplers have been demonstrated experimentally, but the electromagnetic coupling has been found to change significantly with increasing frequency [4] [5]. To compensate for this frequency dependence, holes in the separation metal walls have been used to introduce additional coupling mechanism [6]. However, the use of these holes increases the fabrication difficulty, and accurate modelling of the hole coupling is complicated. In this paper, the use of a dielectric layer over the parallel coupled IDGs is proposed to shorten the length required for the 3–dB coupling and to achieve very wide band for the flat coupling. This new structure is shown in Figure 1, and can be considered as a modification of conventional coupled IDGs by reducing the height of a metal separation wall for the case of $a_1 = 2a_2 + s_2$. This structure is easy to fabricate, and can be accurately analyzed by the full–wave method based on the integral equation formulation and Galerkin's procedure. Results show that the structure exhibits broadband flat coupling characteristics useful for broadband applications to directional couplers.

II. Analysis

Due to the symmetry of the structure with respect to the $x = 0$ plane, the structure is capable of supporting both E_z odd and even modes, and hence only the right–hand half of the cross section need to be considered for the following analysis where time and z dependence $e^{j(\omega t - \beta z)}$ will be omitted for the sake of brevity. Electromagnetic field components can be represented through their Fourier transforms, for instance:
For the air region:

$$E_y(x,y) = \frac{1}{2\pi}\int_{-\infty}^{\infty} \tilde{E}_y(\alpha_0, y)\, e^{-j\alpha_0 x}\, d\alpha_0 \tag{1}$$

For the overlay region:

$$E_y(x,y) = \frac{1}{a_1}\sum_{n=-\infty}^{\infty} \tilde{E}_y(\alpha_{1n}, y)\, e^{-j\alpha_{1n} x} \tag{2}$$

For the right–hand groove region:

$$\begin{aligned} E_y(x',y) &= \frac{1}{a_2}\sum_{n=-\infty}^{\infty} \tilde{E}_y(\alpha_{2n}, y)\, e^{-j\alpha_{2n} x'} \\ &= \frac{1}{a_2}\sum_{n=-\infty}^{\infty} \tilde{E}_y(\alpha^o_{2n}, y)\, e^{-j\alpha^o_{2n} x'} \\ &+ \frac{1}{a_2}\sum_{n=-\infty}^{\infty} \tilde{E}_y(\alpha^e_{2n}, y)\, e^{-j\alpha^e_{2n} x'} \end{aligned} \tag{3}$$

where discrete transform variables α_{1n} and α_{2n} are determined to satisfy the electric field boundary conditions on the sidewalls of the overlay and the right–hand groove. $\alpha_{1n} = \frac{2n\pi}{a_1}, \frac{(2n+1)\pi}{a_1}$ $(n = 0, \pm 1, \pm 2, \cdots)$ for the E_z odd and even modes, respectively. $\alpha_{2n} = \frac{n\pi}{a_2}$, which is divided into two parts: $\alpha^o_{2n} = \frac{2n\pi}{a_2}$ and $\alpha^e_{2n} = \frac{(2n+1)\pi}{a_2}$. The superscript o denotes one part of the fields inside the right–hand groove with the tangential electrical field components E^o_z and E^o_x being odd and even functions of x', respectively. The superscript

0-7803-3246-6/96/$5.00 © IEEE

e stands for the other part with E_z^e and E_x^e being even and odd functions of x', respectively.

The wave equations in the Fourier transform domain are now solved in each region with the application of the boundary condition at the base of the right-hand groove and the radiation condition at infinity. The modal amplitude coefficients in each region are then obtained by introducing the tangential electrical field components E_x^a, E_z^a at the $y = 0$ interface and $E_x^b = E_x^o + E_x^e$, $E_z^b = E_z^o + E_z^e$ at the $y = -h_1$ interface. Next, the relations between tangential magnetic and electric field components at these two interface are obtained in terms of the Fourier transformed Green's functions $[P_i]$ and $[R_i]$ $(i = 0, 1, 2)$. Applying the continuity conditions for the tangential magnetic field components at the $y = 0$ and $y = -h_1$ interfaces results in the following integral equations:

$$\frac{1}{2\pi}\int_{-\infty}^{\infty}\begin{bmatrix} P_0 & 0 \\ 0 & 0 \end{bmatrix}\begin{bmatrix} \tilde{E}_x^a(\alpha_0) \\ \tilde{E}_z^a(\alpha_0) \\ 0 \\ 0 \end{bmatrix} e^{-j\alpha_0 x} d\alpha_0$$

$$+\frac{1}{a_1}\sum_{n=-\infty}^{\infty}\begin{bmatrix} P_1 & R_1 \\ R_1 & P_1 \end{bmatrix}\begin{bmatrix} \tilde{E}_x^a(\alpha_{1n}) \\ \tilde{E}_z^a(\alpha_{1n}) \\ \tilde{E}_x^b(\alpha_{1n}) \\ \tilde{E}_z^b(\alpha_{1n}) \end{bmatrix} e^{-j\alpha_{1n}x}$$

$$+\frac{1}{a_2}\sum_{n=-\infty}^{\infty}\begin{bmatrix} 0 & 0 \\ 0 & P_2 \end{bmatrix}\begin{bmatrix} 0 \\ 0 \\ \tilde{E}_{x'}^o(\alpha_{2n}^o) \\ \tilde{E}_z^o(\alpha_{2n}^o) \end{bmatrix} e^{-j\alpha_{2n}^o x'}$$

$$+\frac{1}{a_2}\sum_{n=-\infty}^{\infty}\begin{bmatrix} 0 & 0 \\ 0 & P_2 \end{bmatrix}\begin{bmatrix} 0 \\ 0 \\ \tilde{E}_{x'}^e(\alpha_{2n}^e) \\ \tilde{E}_z^e(\alpha_{2n}^e) \end{bmatrix} e^{-j\alpha_{2n}^e x'} = 0 \qquad (4)$$

where the Fourier transforms of tangential electric field components at these two interfaces are obtained as follows:

$$\tilde{E}_x^a(\alpha_{1n}) = \int_{-\frac{a_1}{2}}^{\frac{a_1}{2}} E_x^a(x) e^{j\alpha_{1n}x} dx \qquad (5)$$

$$\tilde{E}_z^a(\alpha_{1n}) = \frac{j}{\alpha_{1n}}\int_{-\frac{a_1}{2}}^{\frac{a_1}{2}} \frac{\partial E_z^a(x)}{\partial x} e^{j\alpha_{1n}x} dx \qquad (6)$$

$$\tilde{E}_{x'}^{o,e}(\alpha_{2n}^{o,e}) = \int_{-\frac{a_2}{2}}^{\frac{a_2}{2}} E_{x'}^{o,e}(x') e^{j\alpha_{2n}^{o,e}x'} dx' \qquad (7)$$

$$\tilde{E}_z^{o,e}(\alpha_{2n}^{o,e}) = \frac{j}{\alpha_{2n}^{o,e}}\int_{-\frac{a_2}{2}}^{\frac{a_2}{2}} \frac{\partial E_z^{o,e}(x')}{\partial x'} e^{j\alpha_{2n}^{o,e}x'} dx' \qquad (8)$$

and for the E_z odd modes,

$$\tilde{E}_{x,z}^b(\alpha_{1n}) = 2\cos\frac{\alpha_{1n}(s_2+a_2)}{2}\tilde{E}_{x',z}^o(\alpha_{1n}) + 2j\sin\frac{\alpha_{1n}(s_2+a_2)}{2}\tilde{E}_{x',z}^e(\alpha_{1n}) \qquad (9)$$

For the E_z even modes, cos and j sin in the above equation are replaced by j sin and cos.

Galerkin's procedure is applied to integral equations in (4) to solve for the propagation constants of discrete modes. In (5) – (8), $\frac{\partial E_z^a(x)}{\partial x}$ and $\frac{\partial E_z^{o,e}(x')}{\partial x'}$ are used instead of $E_z^a(x)$ and $E_z^{o,e}(x')$. Because $\frac{\partial E_z^a(x)}{\partial x}$ and $\frac{\partial E_z^{o,e}(x')}{\partial x'}$ satisfy the same boundary and singular edge conditions as $E_x^a(x)$ and $E_{x'}^{o,e}(x')$ respectively, the basis functions for $\frac{\partial E_z^a(x)}{\partial x}$ and $\frac{\partial E_z^{o,e}(x')}{\partial x'}$ can be chosen to be the same as those for $E_x^a(x)$ and $E_{x'}^{o,e}(x')$ respectively. Here Gegenbauer polynomials are chosen as basis functions since their weight function fits the singularity of order $r^{-\frac{1}{3}}$ at the rectangular metal corners [2].

Since there are two parallel grooves coupled tightly by connection with an overlay, there exists a certain frequency range over which only the first E_z even and odd modes can propagate. In this range the characteristics of these two modes can be used to realize a directional coupler. Once the propagation constants of the two modes are found, their difference $(\beta_e - \beta_o)$ can be used to calculate scattering parameters for this coupler with length of L, or the coupling length L_{3dB} for a 3-dB directional coupler [7].

III. Results

To verify the accuracy of the analysis, computed results for the special case where h_1 approaches zero are compared with measured data reported in [4] and [5]. The comparison is shown in Figure 2. Clearly, very good agreement is obtained for propagation constants of the dominant E_z even and odd modes. There is also reasonable agreement for the coupling coefficient.

Figure 3 shows difference between the propagation constants of the dominant E_z even and odd modes and length for the 3-dB coupling as a function of frequency for different values of h_1. As expected, when h_1 increases, the difference increases due to more interaction between these two guides. As a result, the coupling increases and hence the length required for the 3 dB coupling is reduced. It is more interesting to note that as h_1 increases, the difference becomes flatter over the frequency range shown here. This results in flatter coupling. To clearly illustrate this, in Figure 4 coupling coefficient $|S_{31}|$ of the dominant E_z even and odd modes of the coupled IDG section is shown as a function of frequency for different values of h_1. For h_1 =0.1 mm, The coupling $|S_{31}|$ changes rapidly as frequency increases. In fact, the coupling at lower end of the frequency range is about 3.5 dB higher than that at higher end. However, as h_1

increases up to 2.65 mm, the coupling decreases at the lower end and increases at the higher end, respectively. Therefore flatter coupling is achieved. Figure 5 shows scattering parameters of the dominant E_z even and odd modes of the coupled IDG section as a function of frequency for h_1 =2.65 mm. It can be seen that the flat coupling is obtained for a wide range of frequency. For L =139 and 141 mm, we can obtain the bandwidth of 35% (from 7.93 to 11.33 GHz) and 46% (from 7.55 to 12.05 GHz) for the coupling variation of $\pm$0.15 dB and $\pm$0.25 dB, respectively. It is also important to note that for latter band, all the higher order modes are cut off. When h_1 is increased to be higher than 2.65 mm, further improvement in the coupling flatness will be achieved, but the second E_z even mode will begin to appear in the band. It has been found that if the width a_2 of each guide is reduced, the cutoff frequency of the second E_z even mode gets higher, resulting in the wider fundamental-mode bandwidth. Therefore, by further increasing h_1 along with the reduction in a_2, the useable bandwidth for the 3 ± 0.15 dB or 3 ± 0.25 dB coupling, during which only first E_z even and odd modes can propagate, will be further increased.

Figure 6 shows difference between the propagation constants of the dominant E_z even and odd modes and length for the 3-dB coupling for different values of ε_{r1}. As ε_{r1} increases, the difference increases, and hence due to stronger coupling the length for 3 dB coupling decreases. When ε_{r1} is small, the difference decreases generally with increasing frequency. But, when ε_{r1} is large, the difference increases with increasing frequency. Therefore, with suitable choice of ε_{r1}, very flat coupling can be achieved. In fact, the curve for $\varepsilon_{r1} = 6.0$ is seen to be very flat. Figure 7 shows scattering characteristics of the dominant E_z even and odd modes of the coupled IDG section as a function of frequency for ε_{r1} =6.0. For L =165.2 mm, we can obtain the bandwidth of 49% (from 7.0 to 11.5 GHz) for the coupling variation of $\pm$0.15 dB. For L =167.0 mm, the bandwidth of as high as 62% (from 6.7 to 12.75 GHz) can be achieved within the tolerance of $\pm$0.25 dB from the 3 dB coupling.

IV. Conclusion

The integral equation formulation and Galerkin's procedure have been used to analyze the propagation and coupling characteristics of the overlaid parallel coupled IDGs. The accuracy of the analysis has been verified by comparison with available experimental results for one limiting case. Numerical results for propagation constants and scattering parameters have been presented for various values of the thickness and dielectric constant of the overlay. It has been shown that as the thickness and dielectric constant increase, the coupling increases, resulting in shorter length required for the 3-dB coupling. It has also been found that with the suitable choice of these two parameters the IDG coupler shows broadband flat coupling characteristics. In fact, the bandwidth for the two examples has been shown to exceed 45% under the tolerance limit of $\pm$0.25 dB of deviation in coupling from 3 dB. The new guide coupler should be very useful for broadband coupler applications in microwave and millimeter-wave integrated circuits.

References

[1] S. R. Pennock, N. Izzat and T. Rozzi, "Very wideband operation of twin-layer inset dielectric guide," *IEEE Trans. Microwave Theory Tech.*, vol.MTT-40, pp.1910-1917, Oct. 1992.

[2] Z. Fan and S.R. Pennock, "Hybrid mode analysis of parallel coupled inset dielectric guides," *IEE Proc.-Microw. Antenna. Propag.*, vol.142, pp.57-62, Feb. 1995.

[3] Z. Fan and S.R. Pennock, "Broadside coupled strip inset dielectric guide and its directional coupler application," *IEEE Trans. Microwave Theory Tech.*, vol.MTT-43, pp.612-619, March 1995.

[4] S. R. Pennock, D. M. Boskovic and T. Rozzi, "Analysis of coupled inset dielectric guides under LSE and LSM polarization", *IEEE Trans. Microwave Theory Tech.*, vol.MTT-40, pp.916-924, May 1992.

[5] T. Rozzi, S. R. Pennock and D. Boskovic, "Dispersion characteristic of coupled inset dielectric guide", in *Proc. 20th European Microwave Conf.*, 1990, pp.1175-1180.

[6] S. R. Pennock, D. Boskovic and T. Rozzi, "Broadband inset dielectric guide coupler", in *Proc. 21th European Microwave Conf.*, 1991, pp.1142-1147.

[7] J. Miao and T. Itoh, "Hollow image guide and overlayed image guide coupler," *IEEE Trans. Microwave Theory Tech.*, vol.MTT-30, pp.1826-1831, Nov. 1982.

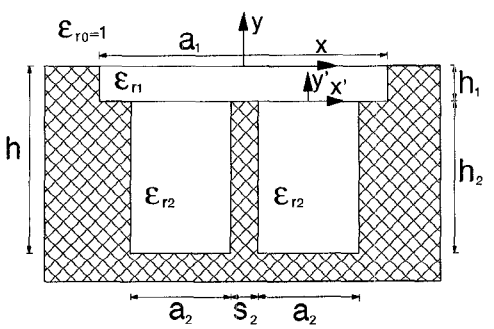

Figure 1: Cross section of the overlaid parallel coupled inset dielectric guides and coordinate systems used in the analysis

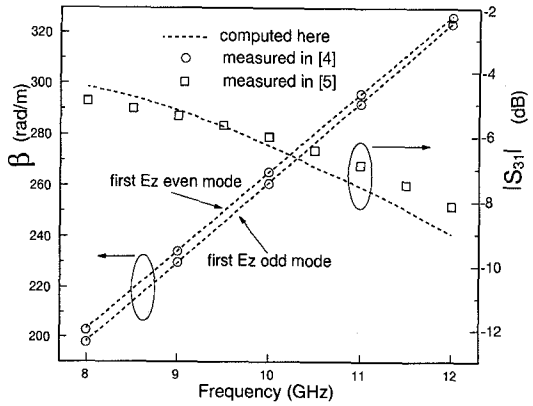

Figure 2: Comparison of propagation constants and coupling coefficient with the measured data reported in [4] and [5] for the case where h_1 approaches zero. (a_1 =22.02 mm, $\varepsilon_{r1} = \varepsilon_{r2}$ =2.04, a_2 =10.16 mm, h =15.24 mm, s_2 =1.7 mm)

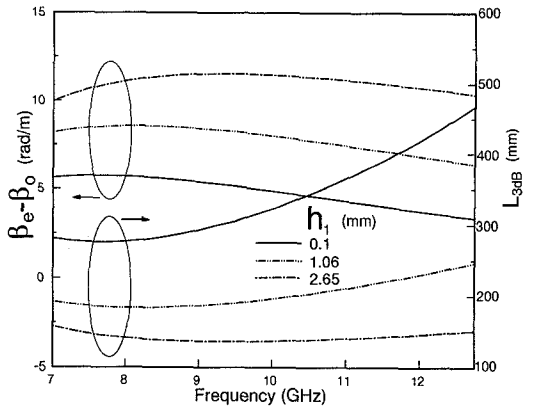

Figure 3: Difference between the propagation constants of the dominant E_z even and odd modes and length for the 3-dB coupling for different values of h_1 (a_1 =16.02 mm, $\varepsilon_{r1} = \varepsilon_{r2}$ =2.04, a_2 =7.16 mm, h =15.24 mm, s_2 =1.7 mm)

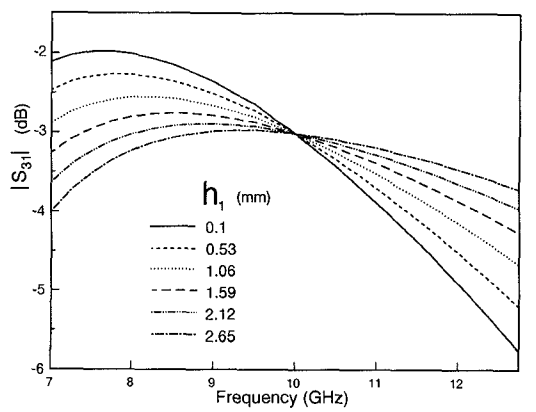

Figure 4: Coupling coefficient of the dominant E_z even and odd modes of the coupled IDG section for different values of h_1 (a_1 =16.02 mm, $\varepsilon_{r1} = \varepsilon_{r2}$ =2.04, a_2 =7.16 mm, h =15.24 mm, s_2 =1.7 mm, $L = L_{3dB}$ at 10 GHz)

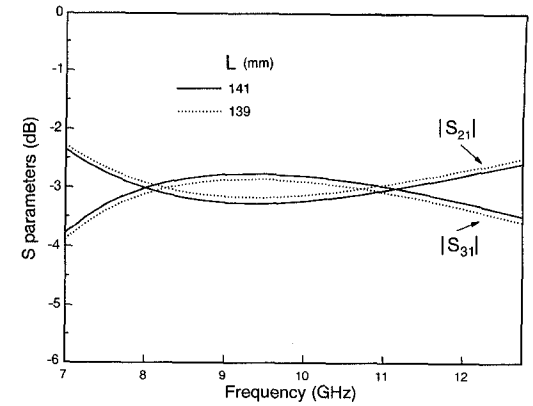

Figure 5: Scattering characteristics of the dominant E_z even and odd modes of the coupled IDG section for h_1 =2.65 mm (a_1 =16.02 mm, $\varepsilon_{r1} = \varepsilon_{r2}$ =2.04, a_2 =7.16 mm, h =15.24 mm, s_2 =1.7 mm)

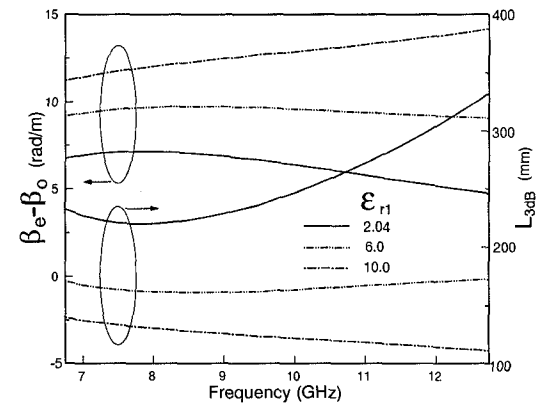

Figure 6: Difference between the propagation constants of the dominant E_z even and odd modes and length for the 3-dB coupling for different values of ε_{r1} (a_1 =16.02 mm, h_1 =0.53 mm, ε_{r2} =2.04, a_2 =7.16 mm, h_2 =14.71 mm, s_2 =1.7 mm)

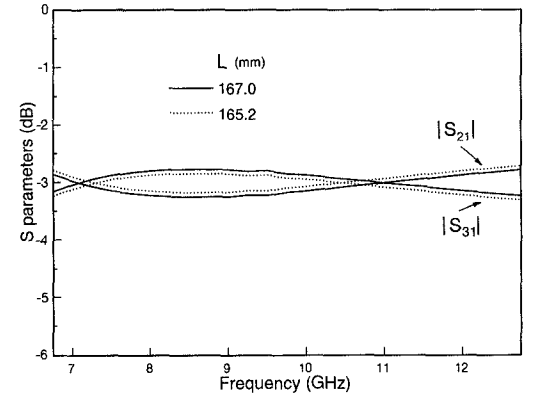

Figure 7: Scattering characteristics of the dominant E_z even and odd modes of the coupled IDG section for ε_{r1} =6.0 (a_1 =16.02 mm, h_1 =0.53 mm, ε_{r2} =2.04, a_2 =7.16 mm, h_2 =14.71 mm, s_2 =1.7 mm)